

## Electronic structure and semiconductor-semimetal transition in InAs-GaSb superlattices

M. Altarelli

Max-Planck-Institut für Festkörperforschung, D-7000 Stuttgart 80, Federal Republic of Germany

(Received 1 March 1983)

Self-consistent electronic structure calculations in the envelope-function approximation are performed for InAs-GaSb superlattices, with a three-band  $\vec{k}\cdot\vec{p}$  formalism and suitable boundary conditions. The subband dispersion for  $\vec{k}$  not parallel to the growth axis, realistically computed for the first time, obeys a no-crossing rule which opens small ( $\leq 10$  meV) gaps between conduction-band-like and valence-band-like subbands. It is therefore argued that the semimetallic behavior observed for periods  $d \geq 180$  Å is dominated by extrinsic effects.

### I. INTRODUCTION

There has recently been much interest in semiconductor superlattices of "type II," such as InAs-GaSb.<sup>1-7</sup> Their characteristic feature is that the top of the GaSb valence band lies higher in energy than the bottom of the InAs conduction band. Charge transfer across each interface of the periodic array and novel electronic properties are to be expected. Experiments,<sup>2-5,8</sup> indeed, indicate a transition from a semiconductor to a semimetal occurring as the superlattice period is increased, and the lowest conduction-band-like subband sinks through the highest heavy-hole-like subband. Therefore, the nature of this transition depends strongly on the superlattice band structure. It is, in fact, well known that in a general low-symmetry direction in  $\vec{k}$  space, no band degeneracies are allowed, so that a gap must appear between the two intersecting bands. The occurrence of the semimetallic state depends, therefore, on the possibility of crossing along high-symmetry directions. A further mechanism takes place if an indirect gap becomes negative, so that pockets of electrons and holes at different points of the Brillouin zone result. This cannot be determined on symmetry grounds, but must be investigated by detailed calculations.

It will be shown in the present paper that neither mechanism is operative in InAs-GaSb superlattices, so that in an intrinsic sample no truly semimetallic band structure results, but rather a zero-gap or very small gap ( $E_g \leq 10$  meV) semiconductor. Therefore, doping and temperature effects must play a key role in the observed semimetallic behavior.

There are some stringent requirements on a band-structure calculation for such systems. In fact, (a) the narrow-gap nature of InAs and GaSb, and the mixing of valence and conduction bands at the interfaces, make a

many-band treatment necessary; (b) the investigation of the bands for  $\vec{k}$  parallel to the layers requires a realistic description of the host bands, and in particular, of the degenerate valence-band edge; (c) the occurrence of charge transfer requires a method suitable for self-consistent calculations. On the other hand, the very large superlattice unit cells in the region of the transition (period  $d \geq 180$  Å) rule out *ab initio* methods<sup>9</sup>; among semiempirical methods, tight-binding theories<sup>1,10</sup> are remarkably simple, but unsuitable for requirement (c) [as well as for (b) if oversimplified schemes are adopted]. The envelope-function approximation appears to be the most convenient framework for this problem, as pointed out by Sham and co-workers<sup>4,11</sup> and by Bastard.<sup>6,7</sup> It is shown in the following that besides fulfilling requirement (a) as pointed out by these authors, this method can be formulated so as to fulfill requirements (b) and (c) as well.

### II. METHOD OF CALCULATION

Consider an *A-B* superlattice composed of layers of thickness *a* and *b*, i.e., with period  $d = a + b$ . Let *x* denote the superlattice axis and let *y, z* denote two orthogonal directions in the  $x = 0$  plane. Following Ref. 11, we choose *z* as the quantization axis of angular momenta, and consider  $\vec{k}$  vectors in the *xy* plane. The six states of the conduction and upper spin-orbit-split valence bands decouple then in two equivalent sets. Our basis is  $u_1 = |s\uparrow\rangle$ ,  $u_2 = |\frac{3}{2}, \frac{3}{2}\rangle$ ,  $u_3 = |\frac{3}{2}, -\frac{1}{2}\rangle$ , and the analogous  $u_4, u_5, u_6$  for the "spin-down" set. We retain the full coupling of the heavy holes with the other bands, which is necessary for a correct description of the dynamics in the layer direction. For  $\vec{k}$  in the (*xy*) plane, the dispersion of spin-up states in material *A*, for example, is given by the eigenvalues of the following matrix (atomic units are used everywhere):

$$H_{jj'}^A = \sum_{\alpha, \beta=x, y} D_{jj'}^{\alpha, \beta} k_\alpha k_\beta + \sum_{\alpha=x, y} P_{jj'}^\alpha k_\alpha + E_j \delta_{jj'}$$

$$= \begin{bmatrix} E_c + \frac{1}{2}k^2 & iP(k_x + ik_y)/\sqrt{2} & -iP(k_x - ik_y)/\sqrt{6} \\ -iP(k_x - ik_y)/\sqrt{2} & E_v - \frac{\gamma_1 + \bar{\gamma}}{2}k^2 & (\sqrt{3})\bar{\gamma}(k_x - ik_y)^2/2 \\ iP(k_x + ik_y)/\sqrt{6} & (\sqrt{3})\bar{\gamma}(k_x + ik_y)^2/2 & E_v - \frac{\gamma_1 - \bar{\gamma}}{2}k^2 \end{bmatrix}, \quad (1)$$

where  $E_c(E_v)$  is the conduction- (valence-) band-edge energy,  $P$  is Kane's momentum matrix element,<sup>12</sup>  $iP = \langle s | p_x | x \rangle$ , and  $\gamma_1$  and  $\bar{\gamma}$  are Luttinger-type valence-band parameters in the spherical ( $\gamma_2 = \gamma_3 = \bar{\gamma}$ ) approximation.<sup>13</sup> The parameters  $P$ ,  $\gamma_1$ ,  $\bar{\gamma}$ , and  $E_c - E_v$  are known, for each material, by magneto-optical experiments.<sup>14,15</sup> The relative position of the band edges of the two materials is, on the other hand, an empirically determined input parameter. By following the standard effective-mass procedure, we obtain equations<sup>4,6-7</sup> for the slowly varying envelope functions  $F_j^{A(B)}(x)$  ( $j=1,2,3$ ) in the form

$$\sum_j [H_{jj'}^{A(B)} + V^{A(B)}(x)\delta_{jj'}] F_j^{A(B)} = E F_j^{A(B)} \quad (j=1,2,3) \quad (2)$$

in the  $A(B)$  part of the superlattice unit cell, respectively. Here  $\vec{k} \rightarrow -i\vec{\nabla}$  in  $H^A$  and  $H^B$ , and  $V^A(x), V^B(x)$  are the potentials arising from charge redistribution across the interfaces.  $F^A$  and  $F^B$  must be joined at the interfaces by suitable boundary conditions. (Similar equations hold, of course, for  $j'=4,5,6$ .) Given the structural similarity of III-V compounds, it is a good approximation<sup>4</sup> to take the basis functions  $u_1 \cdots u_6$  to be the same in  $A$  and  $B$ , which also implies  $P^A = P^B$ . The continuity of the total wave function implies, then, continuity of the envelope function at each interface. The other three boundary conditions<sup>16</sup> are obtained by imposing a constant probability current  $\bar{J}_x(x)$  across all planes perpendicular to  $x$ , and in particular, across the interfaces. Averaging over one unit cell of each material, we find the following for the expectation value of the current operator  $\bar{J}_x$ :

$$\bar{J}_x = \sum_{j,j'} F_j^* [(D_{jj'}^{xy} + D_{jj'}^{yx})k_y + P_{jj'}^x] F_j - i \sum_{j,j'} \left[ F_j^* D_{jj'}^{xx} \frac{\partial}{\partial x} F_{j'} - F_{j'} D_{jj'}^{xx} \frac{\partial}{\partial x} F_j^* \right]. \quad (3)$$

Using the continuity condition, the equality of the  $P$ 's in  $A$  and  $B$ , and the hermiticity of the  $D$  matrices, from the continuity of Eq. (3), we get the following conditions.

$$\sum_{j'} \left[ (D_{jj'}^{xy} + D_{jj'}^{yx})k_y - 2iD_{jj'}^{xx} \frac{\partial}{\partial x} \right] F_{j'} \quad \text{continuous } (j=1,2,3). \quad (4)$$

These boundary conditions reduce, in particular cases, to those derived by other authors: In the absence of  $\vec{k}^2$  terms in the Hamiltonian (vanishing  $D$  matrices) one sim-

TABLE I. Band parameters used in the calculation (from Refs. 4, 14, and 15). The values of  $\gamma_1, \bar{\gamma}$  turn out to be equal within experimental error for both materials, although they need not be.  $\epsilon$  is the dielectric constant, appearing in Poisson's equation for  $V^A, V^B$  (see text).

	InAs	GaSb
$E_c$ (eV)	0.000	0.960
$E_v$ (eV)	-0.420	0.150
$P$ (a.u.)	0.719	
$\gamma_1$ (a.u.)	3.7	
$\bar{\gamma}$ (a.u.)	0.6	
$\epsilon$	15.0	

ply obtains the continuity of the envelopes, as in Ref. 4; the coefficient of the  $\partial/\partial x$  term in Eq. (4) reflects the jump in effective mass that must be included in the derivative continuity condition, as pointed out in Refs. 6 and 7.

Equation (2), for  $A$  and  $B$ , are coupled into a modified variational principle<sup>16,17</sup> which automatically produces solutions satisfying the boundary conditions. From the resulting wave functions, calculated at 21  $\vec{k}$  points in the irreducible portion of the  $(k_x, k_y)$  plane, we calculate the charge-density change, in the  $A$  layers for example, with respect to bulk  $A$  material. This is achieved by considering the  $A$  conduction-band component of all occupied states, and similarly the  $A$  valence-band component of all empty states, which correspond to the excess electron and hole densities, respectively. These components are obtained by projecting, at each  $k$  value, the superlattice wave functions on the eigenvectors of the matrix in Eq. (1), corresponding to the bulk  $A$ -material states. From these  $\rho^A(x)$  and  $\rho^B(x)$ , we obtain  $V^A(x)$  and  $V^B(x)$  in the Hartree approximation<sup>18</sup> by solving Poisson's equation, and iterate to self-consistency. We found six to seven iterations at most to be necessary to stabilize the eigenvalues and potential to better than 1 meV.

We therefore have a scheme which allows us to investigate the subband dispersion in the layer planes realistically and self-consistently for the first time.

### III. RESULTS FOR InAs-GaSb AND DISCUSSION

The parameters used in the calculation for InAs and GaSb are listed in Table I. Figure 1 shows results ob-

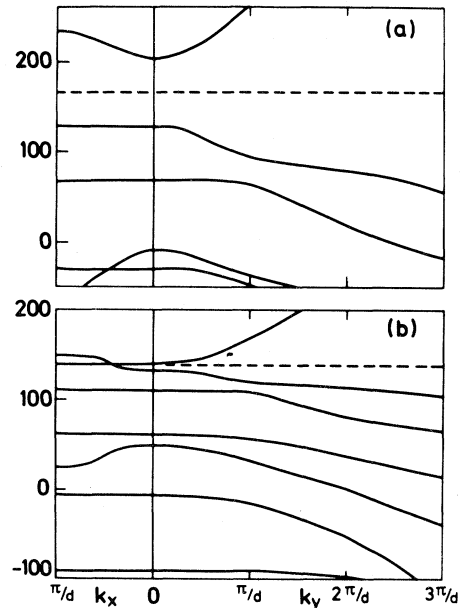


FIG. 1. Band structure of (a) a  $d=2 \times 60 \text{ \AA}$  and (b) a  $d=2 \times 90 \text{ \AA}$  InAs-GaSb superlattice in the flat-band approximation.  $k_x$  is perpendicular to the layers,  $k_y$  parallel to them. The dashed horizontal line denotes the Fermi energy. All energies are in meV.

tained in the non-self-consistent flat-band approximation<sup>4</sup> [ $V^A(x) = V^B(x) = 0$ ], for  $d = 2 \times 60 \text{ \AA}$  and  $d = 2 \times 90 \text{ \AA}$  InAs-GaSb superlattices. These results illustrate a general symmetry principle: Subbands can only cross for  $\vec{k}$  parallel to the superlattice axis  $x$ ; for  $k_y \neq 0$ , hybridization and anticrossing behavior occur.<sup>19</sup> This symmetry principle holds for the Hamiltonian with the spherical approximation [see Eq. (1)], i.e., for an approximation which artificially raises the symmetry of the system. It will *a fortiori* continue to hold in all directions perpendicular to  $k_x$  when the actual, lower symmetry is restored. Thus a gap always opens for  $\vec{k}$  off the  $x$  direction, as is visible in Fig. 1(b). The Fermi surface reduces, for this value of  $d$ , to the one point along  $x$  where the crossing takes place, so that a zero-gap semiconductor, rather than a semimetal, is obtained. When the period is further increased, the crossing electron- and hole-like subbands keep moving along the energy axis in opposite directions, and they are soon completely past each other, resulting in a small-gap semiconductor. This is illustrated in Fig. 2, where the subband structure of a  $d = 120 + 80 \text{ \AA}$  superlattice is shown. Figure 2(b) is in the flat-band approximation. Figure 2(c) is the self-consistent Hartree solution. In Fig. 2(b) the gap is about 10 meV and is along  $\Lambda$ . The substantial quantitative effects of self-consistency [Fig. 2(c)] are such that the gap moves closer to  $L$ , and shrinks to 2 meV; also, the crossing of the two top occupied subbands between  $\Gamma$  and  $L$  disappears. This is because the self-consistent potential raises all states, localized mostly in the InAs layers by  $\sim 10\text{--}15 \text{ meV}$ , and lowers those mostly localized in the GaSb by a comparable amount. About  $\sim 0.9 \times 10^{12} \text{ cm}^{-2}$  electrons are transferred across each interface. The no-crossing rule for  $k_y \neq 0$  is of course preserved, being a consequence of symmetry alone, and so is the resulting strong nonparabolicity of the subbands in both parallel and perpendicular directions.

We have investigated the band structure for many other values of the layer thickness. In no case was a negative indirect gap found, although small positive indirect gaps are present at some thickness values. It appears, therefore, that the indirect gap semimetal case does not apply to InAs-GaSb.

We can compare the results of Fig. 2(c) to those derived from magneto-optical and magneto-transport experiments on a  $d = 120 + 80 \text{ \AA}$  sample.<sup>2,3,5,8</sup> The position of the highest occupied conduction-band-like subband [see Fig. 2(c)] is  $E_1 = 100 \pm 15 \text{ meV}$ ; the first unoccupied subband is  $H_1 = 139 \pm 15 \text{ meV}$ ; the  $\Gamma$ - $L$  bandwidth of  $E_1$  is  $\Delta E_1 = 23 \pm 1 \text{ meV}$ , and the Fermi energy position is given as  $E_F - E_1 = 39 \text{ meV}$ . The results of Fig. 2(c) give  $E_1 = 97 \text{ meV}$ ,  $H_1 = 121 \text{ meV}$ ,  $\Delta E_1 = 15 \text{ meV}$ , and  $E_F - E_1 = 21 \text{ meV}$ . The sensitivity of these numbers to the fine tuning of the input parameters can be shown if we simply take the slightly larger value 0.175 eV (proposed in Ref. 4) in-

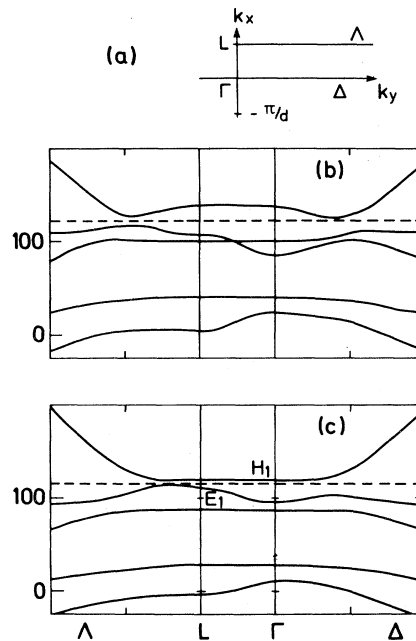


FIG. 2. Band structure of a  $d = 120 + 80 \text{ \AA}$  InAs-GaSb superlattice (b) in the flat-band approximation (c) in the self-consistent Hartree approximation. The Brillouin-zone nomenclature is shown in (a).

stead of 0.150 eV (from Ref. 2) for the position of the GaSb valence-band top; we then obtain  $E_1 = 100 \text{ meV}$ ,  $H_1 = 144 \text{ meV}$ ,  $\Delta E_1 = 19 \text{ meV}$ , and  $E_F - E_1 = 39 \text{ meV}$ , in closer agreement with experiment. It should also be mentioned that the procedure of extracting the experimental values from the actual data implies some assumptions about the structure of the Landau levels which may not be entirely correct for the strong nonparabolicity of the subbands shown in Fig. 2. A full calculation of the energy levels of the superlattice in a magnetic field is currently in progress.<sup>20</sup>

In conclusion, it was shown by explicit self-consistent calculations in the envelope-function approximation that in spite of the peculiar ordering of the energy levels and of the band interchange, no semimetallic band structure is obtained in intrinsic InAs-GaSb. In view of the very small gap values, however, it is to be expected that extrinsic effects produce the semimetallic behavior observed.

#### ACKNOWLEDGMENTS

It is a pleasure to thank A. Fasolino for many useful suggestions, and G. Döhler and E. Tosatti for discussions.

<sup>1</sup>G. A. Sai-Halasz, L. Esaki, and W. A. Harrison, Phys. Rev. B **18**, 2812 (1978).

<sup>2</sup>L. L. Chang, J. Phys. Soc. Jpn. **49**, Suppl. A, 997 (1980).

<sup>3</sup>Y. Guldner, J. P. Vieren, P. Voisin, M. Voos, L. L. Chang, and L. Esaki, Phys. Rev. Lett. **45**, 1719 (1980).

<sup>4</sup>S. R. White and L. J. Sham, Phys. Rev. Lett. **47**, 879 (1981).

<sup>5</sup>J. C. Maan, Y. Guldner, J. P. Vieren, P. Voisin, M. Voos, L. L. Chang, and L. Esaki, Solid State Commun. **39**, 683 (1981).

<sup>6</sup>G. Bastard, Phys. Rev. B **24**, 5693 (1981).

<sup>7</sup>G. Bastard, Phys. Rev. B **25**, 7584 (1982).

- <sup>8</sup>L. L. Chang, N. J. Kawai, G. A. Sai-Halasz, R. Ludeke, and L. Esaki, *Appl. Phys. Lett.* **35**, 939 (1979).
- <sup>9</sup>The only attempt in this direction known to the author [J. Ihm, P. K. Lam, and M. L. Cohen, *Phys. Rev. B* **20**, 4120 (1979)] was limited to periods much smaller than the critical one.
- <sup>10</sup>A. Madhukar, N. V. Dandekar, and R. N. Nucho, *J. Vac. Sci. Technol.* **16**, 1507 (1979).
- <sup>11</sup>G. E. Marques and L. J. Sham, *Surf. Sci.* **113**, 131 (1982).
- <sup>12</sup>E. O. Kane, in *Semiconductors and Semimetals*, edited by R. K. Willardson and A. C. Beer (Academic, New York, 1966), Vol. I, p. 75.
- <sup>13</sup>J. M. Luttinger, *Phys. Rev.* **102**, 1030 (1956).
- <sup>14</sup>C. R. Pidgeon, D. L. Mitchell, and R. N. Brown, *Phys. Rev.* **154**, 737 (1967).
- <sup>15</sup>K. Suzuki and N. Miura, *J. Phys. Soc. Jpn.* **39**, 148 (1975).
- <sup>16</sup>Some of the results of this section are derived with more details by M. Altarelli, in *Applications of High Magnetic Fields in Semiconductor Physics*, edited by G. Landwehr (Springer, Berlin, 1983), p. 174.
- <sup>17</sup>H. Schlosser and P. M. Marcus, *Phys. Rev.* **131**, 2529 (1963), especially Appendix 1.
- <sup>18</sup>For the adequacy of the Hartree approximation, see, e.g., T. Ando, A. B. Fowler, and F. Stern, *Rev. Mod. Phys.* **54**, 437 (1982), Secs. III A and III B.
- <sup>19</sup>The occurrence of this anticrossing behavior was conjectured in Ref. 7.
- <sup>20</sup>A. Fasolino and M. Altarelli (unpublished).